Stanford Exploration Project, Report 93, November 11, 1997, pages 87–111

Stanford Exploration Project, Report 93, November 11, 1997, pages 87–111

Determination of near seafloor properties from ocean-bottom recordings

Christine Ecker [1] *and Colin Sayers* [2]

keywords: *velocity, AVO, inversion, shear wave*

ABSTRACT

We compare two methods of determining the near seafloor parameters (density, P-wave and S-wave velocity) from data recorded by ocean-bottom seismometers (OBS) and ocean-bottom hydrophones (OBH). The first method is based on AVO from ocean-bottom pressure and vertical particle velocity, and the second on AVO from ocean-bottom vertical and radial particle velocity. Using simple synthetic seismograms, we evaluate the parameter estimation for a simple water over half-space model and explore how the results are influenced by layering and poroelastic effects. The method using two particle velocities seems to be more robust and more sensitive to parameter changes over a broader range of angles. Introducing either a 50 m or 100 m thick layer underlaying the seafloor, this method still yields P-wave velocity estimates with errors less than 3% and S-wave velocities with errors less than 7%. The use of pressure and vertical particle velocity does not result in good estimation of P-wave velocity, S-wave velocity or density. In the case of poroelasticity, the pressure-vertical particle velocity method produces reasonably good results for the P-wave velocity ($\leq$ 1% error) and S-wave velocity ($\leq$ 2% error), while introducing a significant error into the density (20% error). Furthermore, poroelasticity has a considerable effect on the radial particle velocity, thus causing the inversion based on the vertical and radial particle velocity components to yield errors of more than 30% for the S-wave velocity estimation.

INTRODUCTION

The determination of near ocean-bottom properties is of significant importance for marine geophysical exploration. P-wave velocity, S-wave velocity and density determine the partitioning of the incident wave field into transmitted P- and S-waves at the seafloor. Furthermore, these parameters are essential inputs for decomposing multi-component seafloor data, as well as for the numerical study of wave propagation

[1] **email**: christin@sep.stanford.edu

[2] Schlumberger Cambridge Research, England, **email**: sayers@cambridge.scr.slb.com

phenomena.

Several methods have been developed in recent years to estimate these near seafloor properties including laboratory measurements on cores, in-situ measurements with probes, and inference from seismic data. The most common seismic techniques are the modeling or the inversion of data recorded by streamer hydrophones in the water layer (Bronston and Graul, 1994; Chapman and Rohr, 1991; Berge et al., 1986; Chapman et al., 1986; Schmidt and Jensen, 1986). Amplitude versus offset (AVO) data contain information about the lithology contrast across an interface and thus provide the means for determining the near seafloor parameters. Recent new developments in acquisition technology make it possible to apply similar techniques to data recorded directly at the ocean bottom by ocean-bottom seismometers (OBS) as well as ocean-bottom hydrophones (OBH). Methods have been proposed to estimate the P- and S-wave velocity and density either from the acoustic/elastic reflection coefficient from point source measurements of pressure and vertical particle velocity component (Amundsen and Reitan, 1995), or to estimate P-wave and S-wave velocity from the vertical and radial particle velocity component measured at the seafloor (Amundsen and Reitan, 1994). In order to apply these techniques on real data, we must understand how factors such as layering or poroelasticity might influence the seafloor parameter inversion, and how robust the methods are under various conditions.

In this paper, we compare the two techniques of seafloor parameter estimation based on (1) AVO from ocean-bottom pressure and vertical particle velocity data and (2) AVO from ocean-bottom vertical and radial particle velocity data. We perform a sensitivity analysis of both methods for the parameters for which we are inverting. Furthermore, we construct simple synthetic seismograms and explore the effect of layering and poroelasticity on the parameter inversion. Subsequently, we draw conclusions about the robustness and preciseness of the two methods under different starting conditions.

AVO TECHNIQUES

Recent developments in acquisition technology make it possible to record data directly at the seafloor by using ocean-bottom seismometers (OBS) and ocean-bottom hydrophones (OBH). This acquisition technique leaves the receiver fixed on the seafloor while the ship moves with the source or leaves the source fixed and moves the receivers. The near sea-bottom properties can be determined by means of either the pressure and vertical particle velocity or the vertical and radial particle velocity.

AVO from pressure and vertical particle velocity

The near seafloor parameters can be determined through the reflection coefficient at the fluid/solid interface. Amundsen and Reitan (1995) have shown that the reflection coefficient can be calculated by spectral division of the pressure and vertical particle velocity of the direct wave and primary reflection transformed to the frequency-radial wavenumber $(\omega - k)$ domain. The data can be transformed to the $(\omega - k)$ domain by applying a Fourier transform with respect to time and a Hankel transform of order 0 with respect to offset (Amundsen, 1993). The reflection coefficient can then be expressed as:

$$R_{calc} = \frac{P(z_1) - \frac{\rho_1}{q_{v_{p1}}} V_z(z_1)}{P(z_1) + \frac{\rho_1}{q_{v_{p1}}} V_z(z_1)} \tag{1}$$

where $P = P(\omega, k)$ is the pressure component and $V_z = V_Z(\omega, k)$ is the vertical particle velocity component. Both of them are measured at the seafloor, whose depth is given by z_1. The vertical slowness is given by $q_{v_{p1}} = \sqrt{v_{p1}^{-2} - p^2}$ and p is the radial slowness given as $p = k/\omega = sin\alpha_1/v_{p1}$. The angle of incidence is given by α_1, and the horizontal wavenumber by k. Each combination of k and ω of the transformed data corresponds to a specific slowness p.

The density, P-wave, and S-wave velocity of the near seafloor can then be determined by inversion. This requires minimization of the difference between the calculated and theoretical reflection coefficient. The theoretical reflection coefficient for plane waves incident at a fluid/solid interface can be described as (Berkhout, 1987):

$$R_{pp} = \frac{A_1\, \rho_2\, q_{v_{p1}} + A_2\, q_{v_{p1}}\, q_{v_{p2}} - \rho_1\, q_{v_{p2}}}{A_1\, \rho_2\, q_{v_{p1}} + A_2\, q_{v_{p1}}\, q_{v_{p2}} + \rho_1\, q_{v_{p2}}} \tag{2}$$

where $A_1 = (1 - 2\, p^2\, v_{s2}^2)^2$ and $A_2 = 4\, p^2\, v_{s2}^4\, \rho_2\, q_{v_{s2}}$ are shear coefficients, $q_{v_{p1}} = \sqrt{{v_{p1}}^{-2} - p^2}$, $q_{v_{p2}} = \sqrt{{v_{p2}}^{-2} - p^2}$ and $q_{v_{s2}} = \sqrt{{v_{s2}}^{-2} - p^2}$ are the vertical P- and S-wave slownesses in the fluid and solid, and $p = \sin\alpha_1/v_{p1}$ is the horizontal slowness.

AVO from vertical and horizontal particle velocity at the seafloor

Instead of using the pressure and vertical particle velocity component, the near seafloor properties can also be determined by using the vertical and radial particle velocity components. As before, this technique requires the transformation of the direct wave components into the frequency-radial wavenumber domain. The Hankel transform is used with n=0 for the vertical velocity component and n=1 for the radial component, yielding V_z and V_r.

Amundsen and Reitan (Amundsen and Reitan, 1994) have derived a medium-dependent AVO relationship between the two field components in the $\omega - k$ domain which can be used to estimate the P-wave and S-wave velocity of the sediments. The "AVO coefficient" determined directly from the data is given by:

$$R_{calc} = \frac{i\,V_r(z_1) + V_z(z_1)}{i\,V_r(z_1) - V_z(z_1)} \tag{3}$$

where $V_r = V_r(\omega, k)$ is the radial particle velocity and $V_z = V_z(\omega, k)$ is the vertical partcle velocity. As before, both of them are measured at the seafloor. The depth of the seafloor is expressed by z_1. The theoretical "AVO coefficient" as derived by Amundsen and Reitan (Amundsen and Reitan, 1994) satisfies the following relationship:

$$R = \frac{p\,(1 - 2\,v_{s2}^2\,(p^2 + q_{v_{p2}}\,q_{v_{s2}})) - q_{v_{p2}}}{p\,(1 - 2\,v_{s2}^2\,(p^2 + q_{v_{p2}}\,q_{v_{s2}})) + q_{v_{p2}}} \tag{4}$$

where $p = \frac{k}{\omega}$ is again the radial slowness and $q_{v_{p2}}$ and $q_{v_{s2}}$ are the P- and S-wave vertical slownesses given by $q_{v_{p2}} = \sqrt{v_{p2}^{-2} - p^2}$ and $q_{v_{s2}} = \sqrt{v_{s2}^{-2} - p^2}$. When $p = 0$ and $p = v_{p2}^{-1}$ (at the critical angle), the AVO coefficient becomes $R = -1$ and $R = 1$, respectively.

Given a combination of AVO coefficients for different radial slownesses, the P-wave and S-wave velocity can be estimated by minimizing the misfit between the theoretical coefficient and the calculated one. Notice that this AVO coefficient is not the same as the reflection coefficient described in the previous sections. While the pressure and vertical velocity data recorded at the seafloor yield a reflection coefficient which depends on density, P-wave, and S-wave velocity of the near seafloor sediments, the vertical and radial components measured at the seafloor yield an AVO relation which depends only on the P-wave and S-wave velocity of the sediments.

SENSITIVITY ANALYSIS

Before attempting to invert for the near seafloor sediment properties, we examine the sensitivity of the reflection coefficient and the AVO coefficient. The water properties will be given by $v_{p1} = 1500$ m/s and $\rho_1 = 1050$ kg/m^3. The near seafloor layer parameters used in this study are $v_{p2} = 1693$ m/s, $v_{s2} = 437$ m/s, and $\rho_2 = 1900$ kg/m^3.

Parameter sensitivity of the reflection coefficient

In this first section, we demonstrate the sensitivity of the reflection coefficient to changes in P-wave velocity, S-wave velocity and density. In each case, one of the parameters was varied while the other two were kept constant. Similar studies have been done by Chapman and Rohr (Chapman and Rohr, 1991) and Amundsen and Reitan (Amundsen and Reitan, 1995).

Figure 1 shows the sensitivity of the reflection coefficient to derivations of the original P-wave velocity (1693 m/s) by ± 100 m/s. The coefficient is very sensitive to P-wave velocity changes near the critical angle ($R = 1$). An increase in v_p shifts the critical angle to smaller angles of incidence. Furthermore, the higher v_p, the higher the reflection coefficient for vertical incident waves.

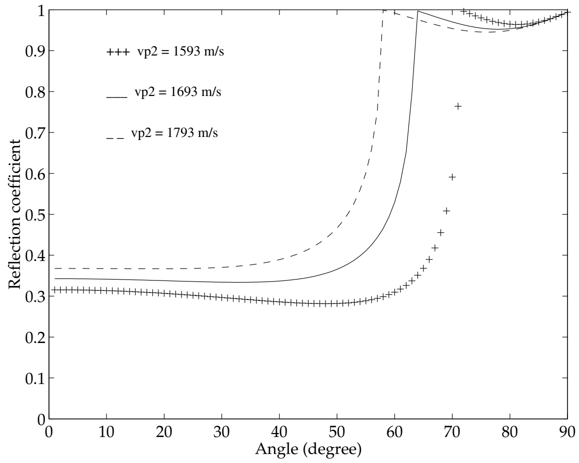

Figure 1: Reflection coefficient for P velocity variations of ± 100 m/s. christine1-refp [NR]

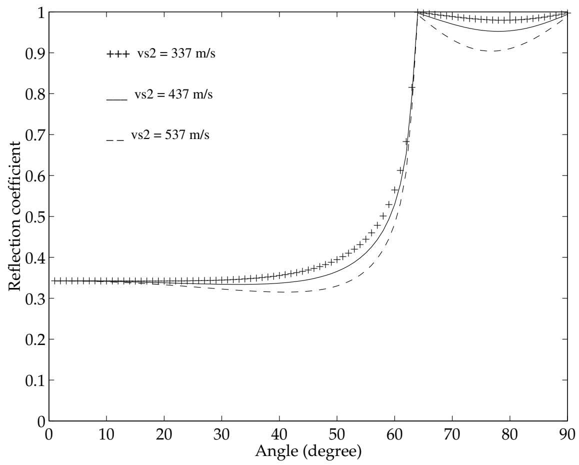

Figure 2: Reflection coefficient for S velocity variations of ± 100 m/s christine1-refs [NR]

The sensitivity to variations in S-wave velocity is shown in Figure 2. The velocity varies from the original sediment velocity of 437 m/s by ± 100 m/s. In contrast to the P-wave velocity sensitivity, the reflection coefficient is only slightly sensitive to changes in v_s for angles less than the critical angle. A considerable dependence on the S-wave velocity exists for post-critical angles, however.

Figure 3 displays the sensitivity to density variations of ± 100 kg/m^3. The reflection coefficient is only sensitive to the density variations until close to the critical angle. The higher the density, the larger the pre-critical reflection coefficient.

When the data include post-critical reflections, the critical reflection angle will determine the P-wave velocity, the post-critical reflections the S-wave velocity, and the small angles of incidence the density.

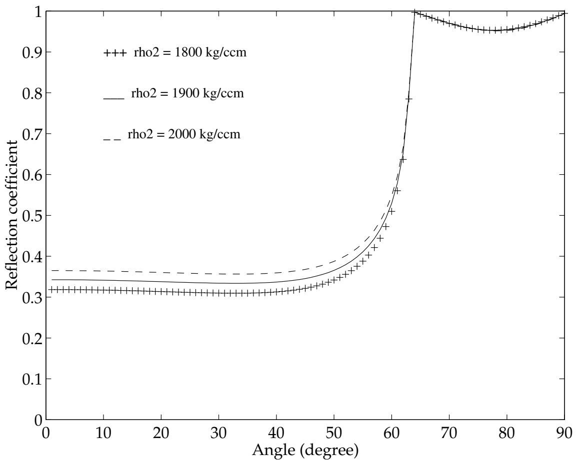

Figure 3: Reflection coefficient for density variations of $\pm$ 100 kg/m^3. christine1-refrho [NR]

Parameter sensitivity of the AVO coefficient

In this section we demonstrate the sensitivity of the AVO coefficient derived from the vertical and radial particle motion to variations in P-wave and S-wave velocity. As before, one of the velocities was varied by $\pm$ 100 m/s, while the other was kept constant. A similar study has been performed by Amundsen and Reitan (Amundsen and Reitan, 1994).

Figure 4 shows the sensitivity of the AVO coefficient to variations in the P-wave velocity. There is a significant sensitivity to changes in v_p at all angles of incidence. The higher the P-wave velocity, the smaller the angle at which the AVO coefficient reaches its minimum value of zero and the smaller the critical angle ($R = 1$).

In Figure 5 we show the sensitivity of the AVO coefficient to variations in the S-wave velocity. At post-critical angles of incidence, there is a significant sensitivity to changes in v_s. The higher the S-wave velocity the smaller the AVO coefficient. There is also a considerable dependence on the S-wave velocity at pre-critical angles of incidence. Close to the critical angle, however, the AVO coefficient barely changes with variations in the S-wave velocity. This is due to the fact that R is independent to v_{s2} at the critical angle.

Since the AVO coefficient is significantly sensitive to both P- and S-wave velocity before the critical angle, both parameters can be estimated for relatively small angles of incidence. However, it has to be taken into account that the radial velocity component will vanish at very small angles of incidence. Thus, the angular coverage should not be too small.

INVERSION OF SYNTHETICS: WATER OVER HALF-SPACE

In this section we compare the two AVO techniques for determining the near sea-floor parameters by using a simple model of 120 m of water overlying a half-space. In this

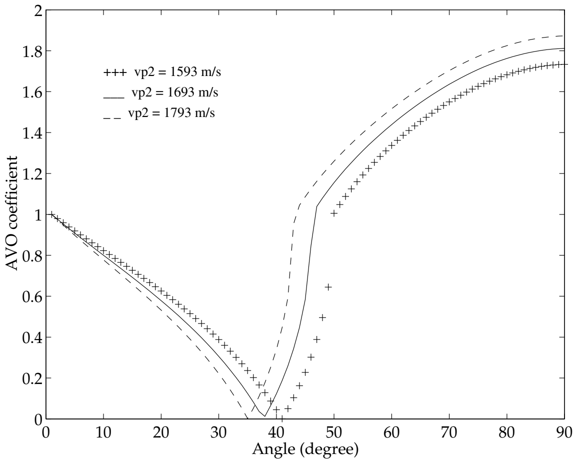

Figure 4: AVO coefficient for P velocity variations of ± 100 m/s. christine1-ref2p [NR]

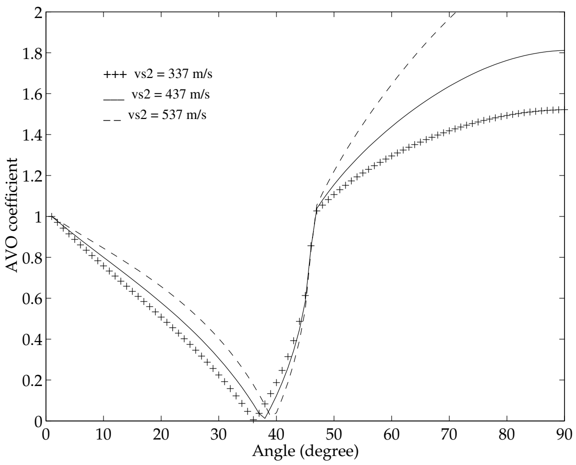

Figure 5: AVO coefficient for S velocity variations of ± 100 m/s. christine1-ref2s [NR]

case, the direct wave and the primary reflection from the seafloor will be unaffected by reflections from subsurface structure. The acoustic/elastic properties of the model are given by the following table:

layer	v_{p2} (m/s)	v_{s2} (m/s)	ρ_2 (kg/m^3)
water	1500	-	1050
sediment	1693	437	1900

Table 1: Properties of the water and the underlying half-space.

The synthetics were generated with a maximum frequency of 30 Hz and a water depth of 120 m. The offset sampling was 25 m, the zero-offset was 12.5 m and the time sampling was 2 ms. The maximum angle of incidence was 84° and the critical angle was 62°.

Inversion Procedure

The near sea-bottom properties can be estimated using inversion. Since the problem is highly non-linear, we applied an iterative damped least-squares approach (Levenberg, 1944; Marquardt, 1963; Lines and Treitel, 1984) which minimizes the misfit between the amplitude spectrum of the theoretical reflection (equation 2) or AVO coefficient (equation 4) and the calculated one (equation 1 and 3). The misfit function is defined as:

$$F = \frac{1}{2} \sum \left(\sqrt{R_{theo} R^*_{theo}} - \sqrt{R_{calc} R^*_{calc}} \right)^2 \tag{5}$$

The star ($*$) denotes the complex conjugate. R is either the reflection coefficient or the AVO coefficient, depending on the data being used. Because of the nonlinearity of the problem, it is important to make a reasonable initial guess of the parameters. Once the near seafloor parameters have been estimated, they can be used to calculate a predicted reflection or AVO coefficient for all angles of incidence.

Inversion of the pressure and vertical particle velocities

We explored the utility of pressure and vertical particle components recorded directly on the ocean-bottom for the determination of the near seafloor properties. The direct wave and primary reflected signals are transformed into the $(\omega - k)$ domain and the reflection coefficient is obtained by spectral division. Inverting the result for density, P-wave and S-wave velocity yields:

$v_{p2} = 1690$ m/s, $v_{s2} = 487$ m/s, and $\rho_2 = 1951$ kg/m^3.

These results can be compared with those used for generating the model (Table 1). While there is only a 3 m/s discrepancy in the P-wave velocity, the S-wave velocity is off by about 50 m/s ($\approx$ 10% error), and the density by 51 kg/m^3 ($\approx$ 3% error). The amplitude spectrum of the reflection coefficient obtained from the data in the $(\omega - k)$ domain is overlain by the AVO curve calculated from the inversion results and shown in Figure 6. The fit is reasonably good. Figure 7, which displays the theoretical AVO curve and the inverted one, shows these curves to be in good agreement. The largest discrepancy occurs at the post-critical angles, which is caused by the fact that the highest error in the inverted parameters is in the S-wave velocity.

The deviation of real and inverted S-wave velocity results from the scatter in the reflection coefficient. Less information is available for the post-critical reflections, thus causing a larger spread of the reflection coefficient in that region. Furthermore, aperture effects in the Hankel transform, and division by higher frequency vibrations in the data might introduce additional scattering effects. Constraining the inversion by prior information might improve the result, as only two parameters would have to be inverted for.

Next we explored the robustness of the parameter inversion by using less angular information in the inversion. For different maximum angles of incidence, the inversion yields the following results which are listed in Table 2.

Angle (°)	v_{p2} (m/s)	v_{s2} (m/s)	ρ_2 (kg/m^3)
84	1690 - 0.2%	487 + 11.4%	1951 + 2.7%
60	1707 + 0.8%	504 + 15.3%	1916 + 0.8%
50	1673 - 1.2%	453 + 4.7%	1948 + 2.5%
40	1633 - 3.5%	417 - 4.6%	1994 + 5.0%

Table 2: Inverted density, P-wave velocity and S-wave velocity using different maximum angles of incidence. The error with respect to the real values is given in ±%.

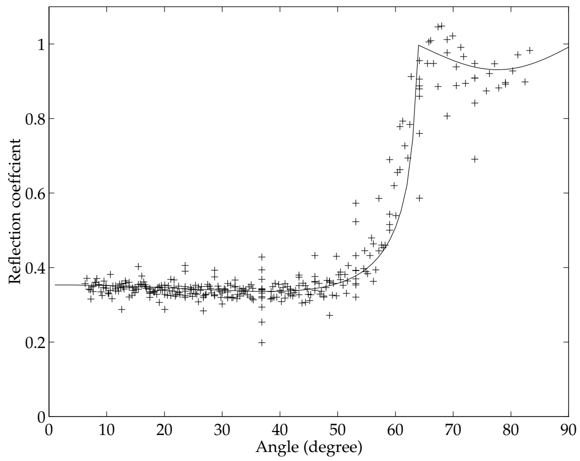

Figure 6: The calculated reflection coefficient from the P-Vz data is represented by +. It is overlain by the AVO curve based on the inverted values. christine1-vzp [NR]

The P-wave and S-wave velocities are estimated with reasonable accuracy for all angles, but the density becomes slightly less well determined with decreasing angles.

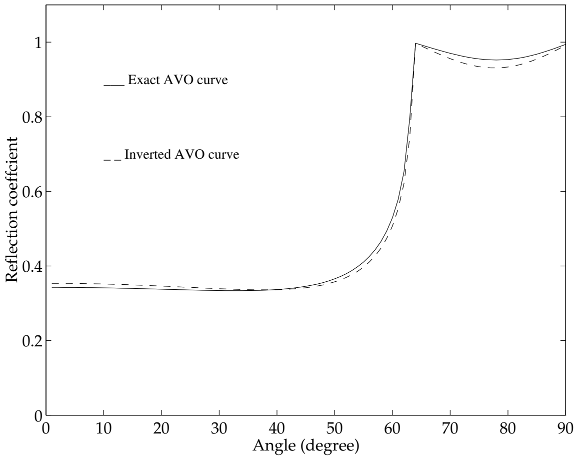

Figure 7: Theoretical AVO curve (solid line) versus inverted curve (dotted line). $\boxed{\text{christine1-vzpavo}}$ [NR]

Even though the sensitivity analysis indicated that most shear wave information is contained in the post-critical reflections, well-constrained data will give good estimates for lower angles. For real data, this method is complicated by the fact that the pressure recording and the vertical particle velocity component have to be calibrated for comparison of the amplitude information.

Inversion of the vertical and horizontal particle velocities

In this section we explore the utility of the vertical and radial particle velocity components measured at the ocean-bottom for the seafloor parameter inversion. The direct wave components are transformed as before into the $(\omega - k)$ domain and the AVO coefficient is determined. Inversion of the data yields the following parameters:

$$v_{p2} = 1689 \text{ m/s and } v_{s2} = 426 \text{ m/s}.$$

As with the previous technique, the P-wave velocity is very well determined. The S-wave velocity is within a 3% error bound. The AVO coefficient determined from the data and the AVO curve based on the inverted values are shown in Figure 8. The data fit is very good. The theoretical AVO curve is compared with the inverted one in Figure 9. It is obvious that they are in good agreement.

Using different maximum angles of incidence, we evaluated again how robust the method is for different angular coverages:

Angle (°)	v_{p2} (m/s)	v_{s2} (m/s)
84	1689 - 0.2%	426 - 2.5%
60	1699 + 0.4%	435 - 0.5%
50	1562 - 7.7 %	328 - 25%
40	1665 - 1.7 %	400 - 8.5%

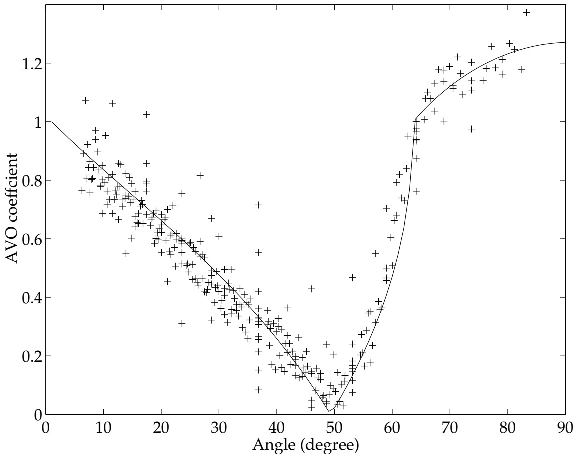

Figure 8: The AVO coefficient calculated from the Vz-Vx data is represented by +. It is overlain by the AVO curve based on the inverted parameters. christine1-vzvx [NR]

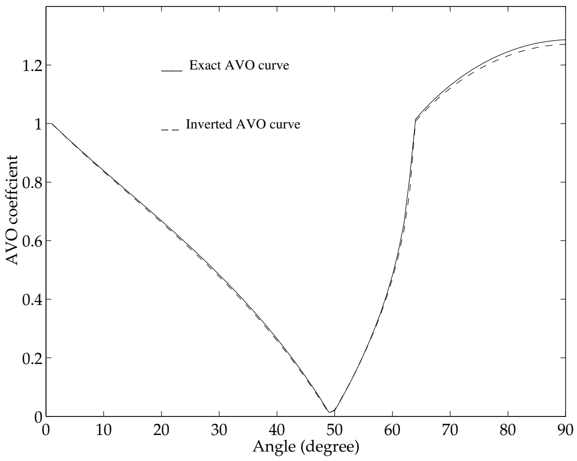

Figure 9: Theoretical AVO curve (solid line) versus inverted one (dotted line). christine1-vzvxavo [NR]

Table 3: Inverted P-wave velocity and S-wave velocity using different maximum angles of incidence. The error with respect to the real values is given in $\pm\%$.

It is obvious that for using a maximum angle of $50°$, the inversion yields rather badly constrained seafloor parameters. This angle of incidence corresponds exactly to where the AVO coefficient determined from the data reaches approximately 0. Otherwise, seafloor parameters estimated from the two particle velocity components seem to be constrained in a much better way than the one estimated using pressure and vertical particle velocity. This is partly due to the fact that the method inverts only for two parameters, thus making it more stable, and that the AVO coefficient is sensitive to the S-wave velocity over a broader range of angles of incidence. Furthermore, the two data components used in these methods do not need to be calibrated prior to the inversion.

INVERSION OF SYNTHETIC DATA: EFFECT OF LAYERING

In this section we examine the effect of layering on the inversion results. Assuming that the near seafloor sediments are underlain by a hard layer will result in interference effects between the signals from the seafloor and the one from the interface between the first and second layer. Using a hard layer simulates the extreme case of subsurface structure effects, and will thus produce upper error bounds for the inverted ocean-bottom parameters. We explore the effects for a layer which is either 100 m or 50 m thick. The synthetics were generated using the same parameters as described in the previous section. The acoustic/elastic properties of the water and the two layers are shown in Table 4.

layer	v_{p2} (m/s)	v_{s2} (m/s)	ρ_2 (kg/m^3)
water	1500	-	1050
1	1693	437	1900
2	2141	781	2100

Table 4: Properties of the water and the two layers underlying the water.

Figures 10, 11, and 12 show the synthetic seismograms for the vertical particle velocity, radial particle velocity and the pressure for the near sea-bottom layer being 100 m thick. In the case of a 50 m thick layer, the interference of the signals will appear at smaller offsets.

Prior to the inversion of the data for the near seafloor parameters, the arrivals of the wave that is being reflected off the second layer were muted out, leaving only the signals generated by the seafloor (Figures 13, 14, 15). Those signals were then transformed into the $(\omega - k)$ domain, in which the reflection and AVO coefficients were determined.

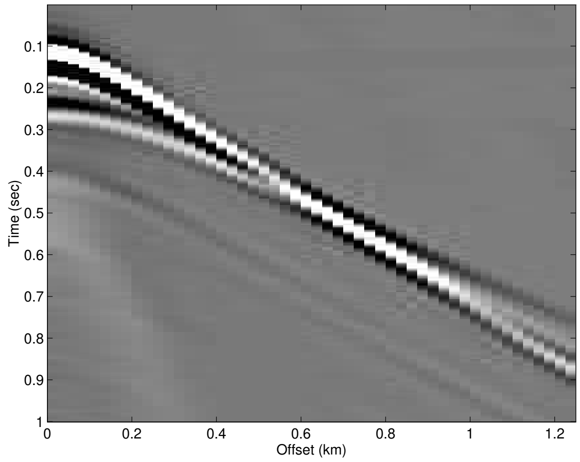

Figure 10: Vertical particle motion for a 100 m thick layer. christine1-layer100 [NR]

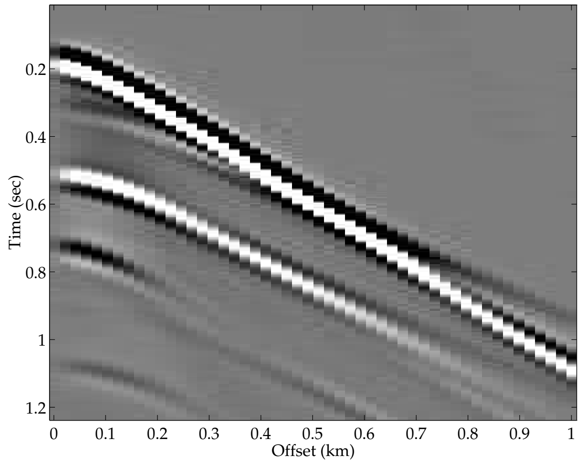

Figure 11: Radial particle motion for a 100 m thick layer. christine1-vxl100 [NR]

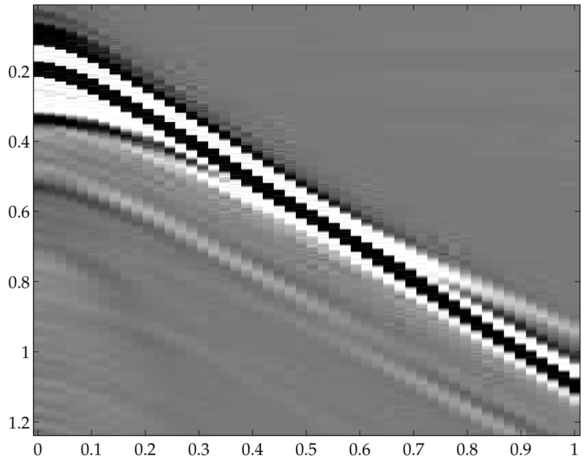

Figure 12: Pressure for a 100 m thick layer. christine1-pl [NR]

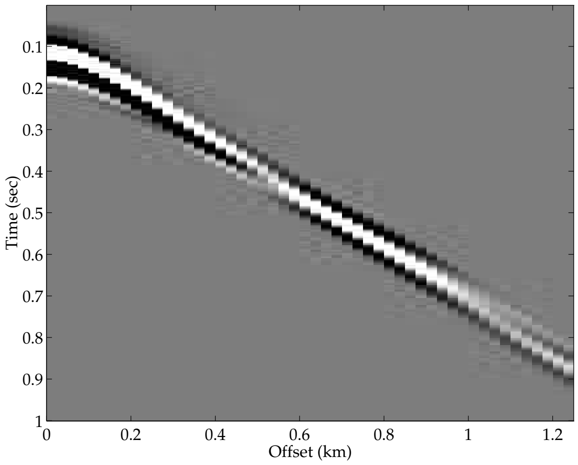

Figure 13: Vertical particle motion for a 100 m thick layer after muting. christine1-vzl [NR]

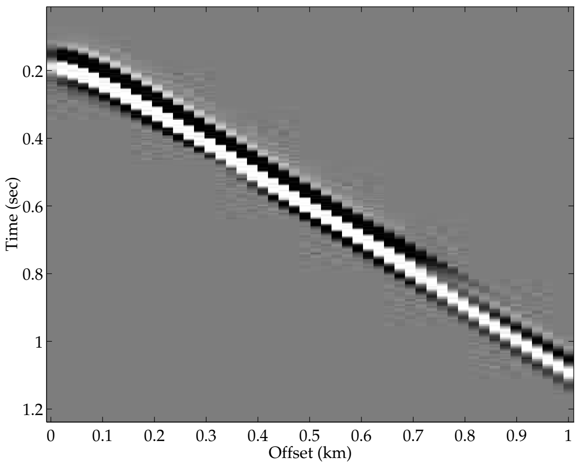

Figure 14: Radial particle velocity for a 100 m thick layer after muting. christine1-vxl100m [NR]

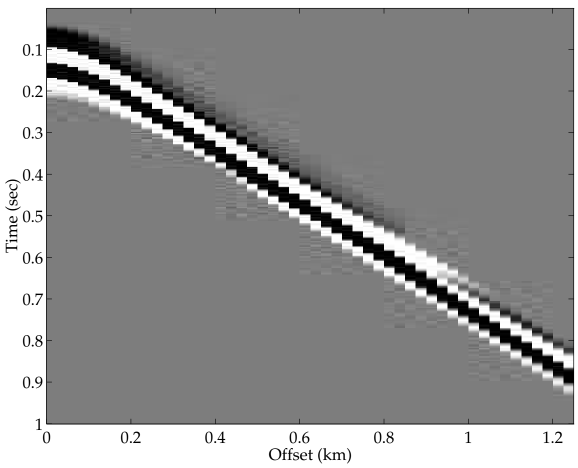

Figure 15: Pressure for a 100 m thick layer after muting. christine1-plm [NR]

Inversion from pressure and vertical velocity data

In this section, we evaluate the effect that layering has on the inversion by means of pressure and vertical particle velocity data. We explored the inversion for the near ocean-bottom parameters in three different ways. First we used the muted data without any changes or constraints to examine the full impact of the layering (case 1). Then we tried to remove the effect of the second layer by using only the first 362 m in offset (case 2). Since the seafloor is at a shallow depth of 120 m, these offsets still allow for an angle coverage above critical angle. Subsequently, we used all offsets again in the data transformation but constrained the inversion by assuming an a priori determined P-wave velocity and by restricting the maximum angle of incidence used in the inversion to 30° - 35° (case 3). The P-wave velocity was set to 1650 m/s which includes an error of 2.5%.

The near sea-floor parameters resulting from the inversion and their error bounds are listed in Table 5.

case	v_{p2} (m/s)	v_{s2} (m/s)
1	1867 + 10.3% / 1912 + 12.9%	483 + 10.5% / 557 +27.5%
2	1742 + 2.9% / 1526 - 9.9%	846 + 93.6% / 373 - 14.6%
3	1650 - 2.5% / 1650 - 2.5%	338 - 22.7%/ 341 - 22%

case	ρ_2 (kg/m^3)
1	1814 - 4.5% / 1849 - 2.7%
2	2228 + 17.3% / 2359 + 24.5%
3	1970 + 3.7% / 1939 + 2.1%

Table 5: Inverted near sea-bottom properties. The left values are for 100 m layering, the right values for 50 m layering.

From the data values alone, it is obvious that the 100 m layering affects the inversion less than the 50 m layering when all data were used (case 1). In both layering cases (100 m and 50 m), the inverted seafloor parameters deviate significantly from the real ones. Using only the near offset data (case 2), we see that the P-wave velocities become more constrained, while the densities become less well constrained. The inverted S-wave velocity shows more than 90% error for the 100 m layering. In the case of a priori P-wave velocity information and a constraining of the inversion to angles less than 35° degrees, both the inversion of the data for 100 m layering and for 50 m layering show comparable results.

Figure 16 displays the reflection coefficient and the inverted AVO curve for the 100 m layering in the case in which all data were used. By comparison, Figure 17 shows the same for 50 m layering. It is obvious that in both cases the calculated reflection coefficient displays considerably more scattering than that without layering effects (see Figure 7). For 100 m layering, the data are significantly affected at angles above 35°. The 50 m layering introduces scattering at smaller angles. In both cases, the critical angle information seems to have been shifted to smaller angles. The scattering occurs at angles at which the seismic signals interfere.

Figures 18 and 19 compare the AVO curves for all three inversion cases with the theoretical one. The constrained inversion results in the best fit, since both the errors in the P-wave velocity and density are rather small. The S-wave velocity was determined best when all the data was used (case 1). In that case, however, P-wave velocity and density deviated too much. For 50 m layering, none of the inverted AVO curves matches the theoretical very well. The best fit was probably achieved by the constrained inversion (case 3).

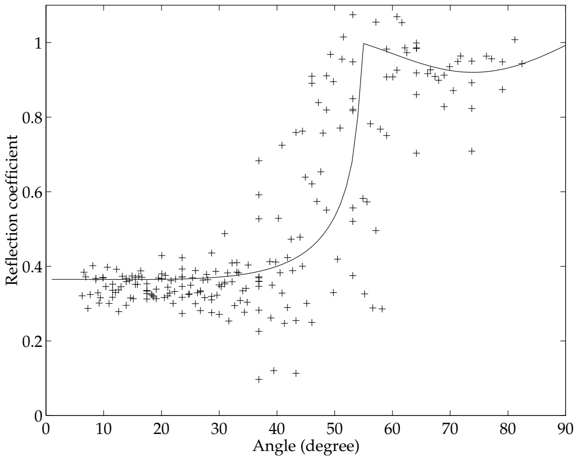

Figure 16: The reflection coefficient calculated from all P-Vz data in the case of 100 m layering is represented by +. The inverted AVO curve is overlain. christine1-vzplavo [NR]

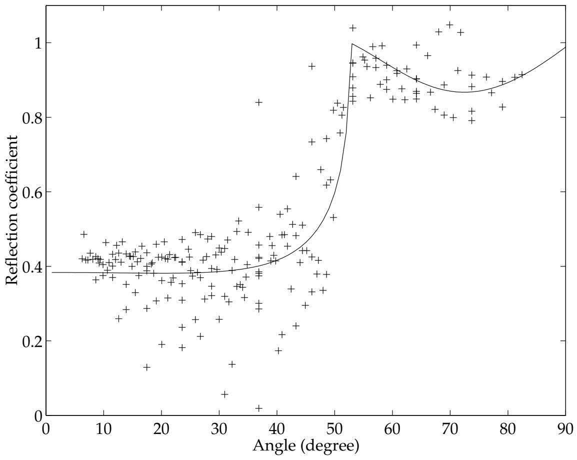

Figure 17: The reflection coefficient calculated from all P-Vz data in the case of 50 m layering is represented by +. The inverted AVO curve is overlain. christine1-vzpl50avo [NR]

Inversion from vertical and radial particle motion

In this section we explore the effect of layering on the inversion using vertical and radial particle velocity. As in the previous section, we first used all the data to examine the full impact of the layering on the data (case 1). Subsequently, we used only the

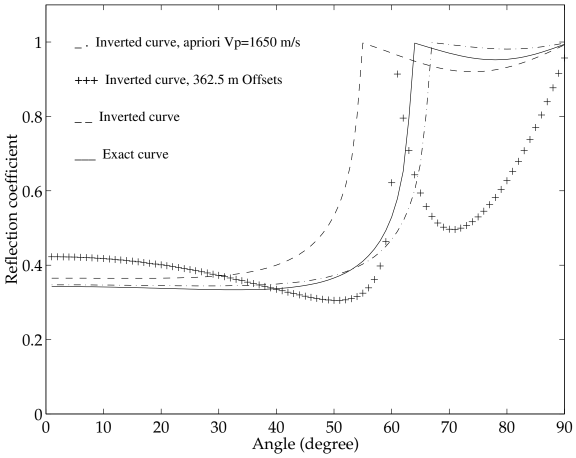

Figure 18: Comparison of the three inverted AVO curves with the exact one in the case of 100 m layering. christine1-100avo [NR]

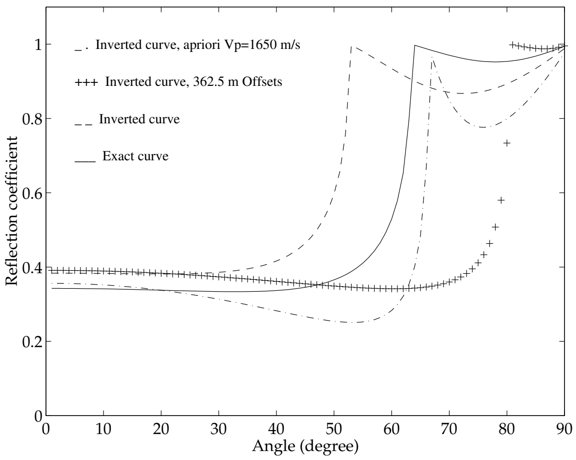

Figure 19: Comparison of the three inverted AVO curves with the exact one in the case of 50 m layering. christine1-50avo [NR]

near offsets (case 2) in an attempt to reduce the layering effect. The inversion results are shown in Table 6.

case	v_{p2} (m/s)	v_{s2} (m/s)
1	2115 + 24.9% / 2125 + 25.5%	315 - 27.9%/ 287 34.3%
2	1660 - 1.9% / 1604 - 2.1%	411 - 5.9% / 464 + 6.2%

Table 6: Inverted near seafloor properties. The left values are for 100 m layering, the right ones for 50 m layering.

The inversion results show that when we use the data only as long as the subsurface structure effects are small (case 2), the P-wave and S-wave velocities are within reasonable error bounds. It can also be noted that when all data are used, the inverted P-wave velocity is very close to the velocity of the second layer. It converges to the velocity of the first layer when the large offset data are neglected.

Figure 20 shows the AVO coefficient for 100 m layering and the inverted AVO curve. Figure 21 displays the same for 50 m layering. In both cases, the AVO coefficient contains significant scattering at angles where the seismic signals from the seafloor and the second layer interfere. Furthermore, the angle at which the AVO coefficient reaches its minimum value of 0 and the critical angle have been shifted (compare with Figure 8).

The inverted AVO curves are compared with the theoretical ones in Figures 22 and 23. It is obvious how well the AVO curves agree both for 100 m layering and 50 m layering when only the near offset data were used.

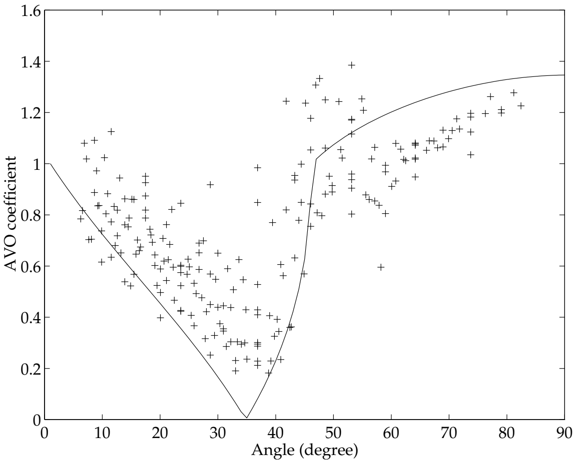

Figure 20: The AVO coefficient calculated from all Vz-Vr data in the case of 100 m layering is represented by +. The inverted AVO curve is overlain. christine1-vzxlavo [NR]

In contrast to the P-Vz method, the Vz-Vx method yields reasonable seafloor parameters when only the near-offset data are used. It seems to be more stable and robust in the case of layering and it affects the inversion less. The use of a very hard second layer simulates the extreme case of layering. If the properties of the layer

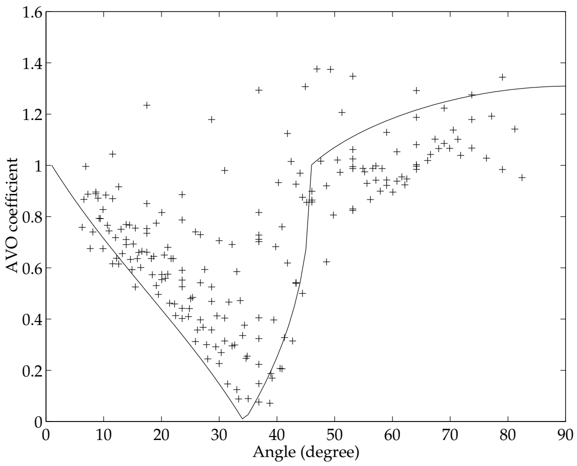

Figure 21: The AVO coefficient calculated from all Vz-Vr data in the case of 50 m layering is represented by +. The inverted AVO curve is overlain. christine1-vzxl50avo [NR]

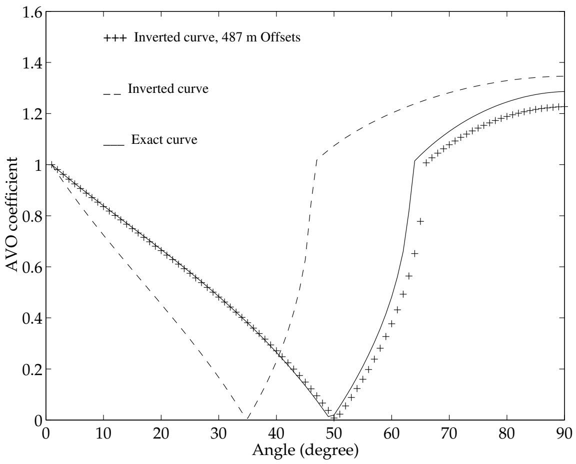

Figure 22: Comparison of the two inverted AVO curves with the exact one in the case of 100 m layering. christine1-100xavo [NR]

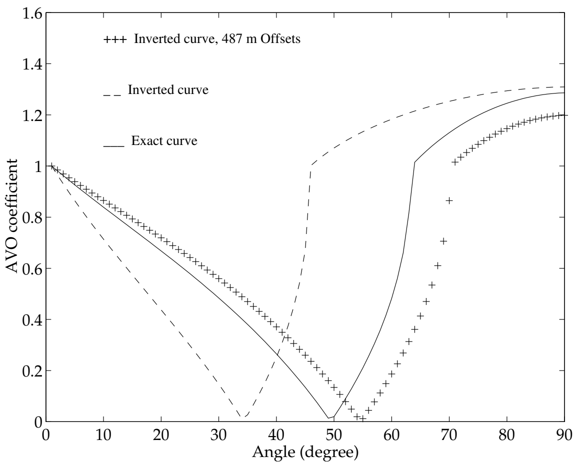

Figure 23: Comparison of the two inverted AVO curves with the exact one in the case of 50 m layering. christine1-50xavo [NR]

are closer to the near sea-bottom ones, the inversion should yield more constrained parameters with fewer errors. It might also be interesting to examine the effect when interference from more than one layer occurs.

INVERSION OF SYNTHETICS: EFFECT OF POROELASTICITY

In this section we determine the effect of poroelasticity on the inversion. Previously, the near seafloor sediment was assumed to be an elastic medium. In reality, however, it is a porous medium whose pores are filled with fluid. In order to evaluate the possible impact on the data and the inversion, synthetics were generated for water overlaying a porous half space. The sediment was assumed to have 46% porosity, thus making it very unconsolidated. The effective parameters for the half-space are given in Table 7.

ϕ	v_{p2} (m/s)	v_{s2} (m/s)	ρ_2 (kg/m^3)
46	1671	430	1891

Table 7: Effective layer properties.

Inversion from pressure and vertical velocity data

We used the pressure and vertical velocity component of the seafloor signal to invert for the near sea-floor parameters. The technique is the same as described before. The data were transformed into the frequency-radial wavenumber domain, the reflection coefficient was calculated and then inverted for the seafloor parameters. The inversion results can be seen in Table 8.

ϕ	v_{p2} (m/s)	v_{s2} (m/s)	ρ_2 (kg/m^3)
46	1661 - 0.6%	440 + 2%	2268 + 19.9%

Table 8: Inverted layer properties.

The inversion results show that the density is less well constrained and has significant errors. P-wave velocity and S-wave velocity are reasonably well determined. Figure 24 displays the theoretical reflection coefficient versus the inverted one. It is obvious that most discrepancy exists at pre-critical angles. This discrepancy is caused by the large error in the density, which mainly controls the near to pre-critical angles (see sensitivity analysis).

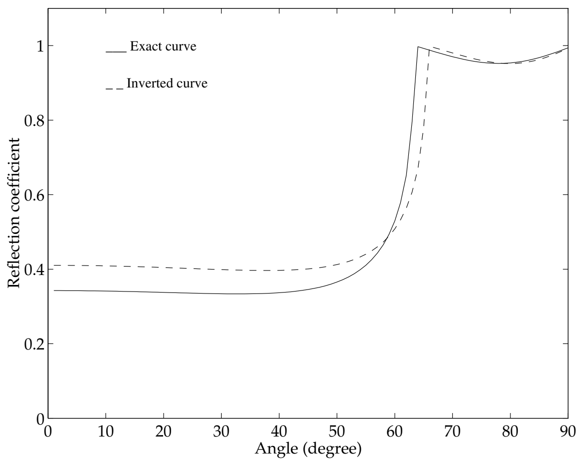

Figure 24: Inverted AVO curve versus exact curve for P-Vz data. christine1-vzpp1avo [NR]

Inversion using vertical and radial particle velocity

In this section we use the vertical and radial particle velocity components of the seafloor signals to invert for the near sea-bottom properties. The inversion results can be found in Table 9.

ϕ	v_{p2} (m/s)	v_{s2} (m/s)
46	1678 + 0.4%	299 - 30.5%

Table 9: Inverted layer properties.

The values show that for both porosities, the P-wave velocity could be determined very well. The S-wave velocities, however, show very large errors.

Figure 25 compares the inverted AVO curve with the theoretical one. The most significant discrepancy occurs at post-critical angles. This region is the most sensitive to changes in the S-wave velocity. The fluid appears to affect the radial particle velocity component in such a strong way that determination of the correct S-wave velocity seems to be impossible.

More work needs to be done to examine this effect of poroelasticity on the data in order to predict the near seafloor parameters. In addition to varying the porosity of the medium, it might be worthwhile to check the effect other parameter variations have.

CONCLUSIONS

We compared two methods of determining the near seafloor parameters from data recorded by OBS and OBH. The first method is based on AVO from pressure and

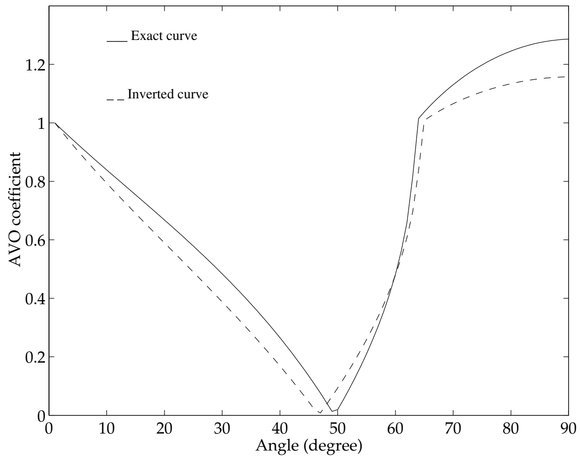

Figure 25: Inverted AVO curve versus exact one for Vz-Vr data. christine1-vzvxp1avo [NR]

vertical particle velocity of the seafloor signals. The second method uses AVO of the vertical and radial particle velocity. Using simple synthetic seismograms, we evaluated the effect of layering and poroelasticity on the parameter inversion.

We can conclude that the method using Vz-Vr seems to be more robust and stable. Reasonable inversion results can be obtained for angular coverage considerably smaller than the critical angle. Furthermore, the two components need not to be calibrated prior to the inversion. In case of layering, the P-Vz method does not result in good estimates for density, P-wave and S-wave velocity. The Vz-Vr method, on the other hand, can still yield a P-wave velocity with an error of 1.9% and an S-wave velocity of 6% when only the near offsets are used in the inversion. Since the effect of layering was simulated with a hard layer, these error bounds are probably upper limits. Layers with parameters closer to the ones of the near seafloor should result in better constrained inversion results.

Poroelasticity has a distinct effect on both reflection and AVO coefficients. The Vz-P method gives good estimates of P-wave velocity ($\leq$ 1% error) and S-wave velocity ($\leq$ 2% error). The density cannot be estimated within small error bounds. The error is about 20%. The Vz-Vr method produces only a good constraint on the P-wave velocity ($\leq$ 1% error). The fluid appears to have a significant effect on the radial component, resulting in strong deviations between the true and inverted S-wave velocity ($\geq$ 30% error). M ore work is required in order to fully understand the effect of poroelasticity on the inversion results.

Finally, we can conclude that the Vz-Vr method seems to be superior to the P-Vz method for the determination of the near seafloor parameters. It appears to be more stable and robust even in the case of layering.

ACKNOWLEDGMENTS

We would like to thank Schlumberger Cambridge Research for a great and productive research environment with excellent personal and computer resources. The paper was the result of a summer internship of Christine Ecker with SCR this summer. We would also like to thank Chris Chapman for his helpful discussions about Hankel transforms.

REFERENCES

Amundsen, L., and Reitan, A., 1994, AVO estimation of water-bottom P- and S-wave velocities from the particle velocity field: Jour. Seis. Expl., **3**, 231–243.

Amundsen, L., and Reitan, A., 1995, Estimation of sea-floor wave velocities and density from pressure and particle velocity by AVO analysis: Geophysics, **60**, 1575–1578.

Amundsen, L., 1993, Wavenumber-based filtering of marine point-source data: Geophysics, **58**, 1335–1348.

Berge, A. M., Drivenes, G., Kanestrom, R., and Beskow, B., 1986, Acoustic modeling of the seafloor: Geophys. Prosp., **34**, 11–29.

Berkhout, A. J., 1987, Applied seismic wave theory: Elsevier.

Bronston, M. A., and Graul, J. M., 1994, The determination of shallow marine sediment lithology using high-resolution multi-offset seismic data: Offshore Technology Conference, 31–41.

Chapman, N. R., and Rohr, K., 1991, Measurement of the elastic properties of the ocean bottom by inversion of reflection amplitude data: Shear Waves in Marine Sediment, 537–544.

Chapman, R., Levy, S., Cabrera, J., Stinson, K., and Oldenburg, D., 1986, The estimation of the density, P-wave, and S-wave speeds of the top most layer of sediments, from water bottom reflection arrivals: Ocean Seismo-Acoustics, 703–710.

Levenberg, K., 1944, A method for the solution of certain nonlinear problems in least squares: Quarterly App. Math., **2**, 164–168.

Lines, L. R., and Treitel, S., 1984, Tutorial: A review of least-squares inversion and its application to geophysical problems: Geophys. Pros., **32**, 159–186.

Marquardt, D. W., 1963, An algorithm for least squares estimation of nonlinear parameters: Jour. Soc. Ind. App. Math., **11**, 431–441.

Schmidt, H., and Jensen, F. B., 1986, Evaluation of experimental techniques for determining the plane wave reflection coefficient at the sea floor: Ocean Seismo-Acoustics, 721–730.